g Tensor and Spin Density of the Modified Tyrosyl Radical in Galactose Oxidase: A Density Functional Study

Martin Kaupp,*,† Tobias Gress,† Roman Reviakine,‡ Olga L. Malkina,‡ and Vladimir G. Malkin‡

Institut für Anorganische Chemie, Universität Würzburg, Am Hubland, D-97074 Würzburg, Germany, and Institute of Inorganic Chemistry, Slovak Academy of Sciences, Dubravska Cesta 9, SK-84236 Bratislava, Slovakia

Received: July 24, 2002; In Final Form: October 25, 2002

The influence of ortho sulfur substitution in the modified tyrosyl radical in apo-galactose oxidase on the **g** tensor and the spin-density distribution has been studied by calculations on various model systems using an accurate DFT approach. Computed **g** tensors agree well with experimental observation, and they are intermediate between the extremely large substituent effect found in a previous DFT study and the very small changes found in MCSCF calculations. The origin of the substituent effects has been studied by fragment analyses of the spin−orbit/orbital-Zeeman **g**-tensor contributions, and it is discussed in relation to the spin-density distributions. The influence of hydrogen bonding on **g** tensors is studied by appropriate model complexes with water. Further calculations on radicals including heavier chalcogen substituents XH (X = O, S, Se, Te) predict very large g_x and g_y components with selenium- and tellurium-substituted systems due to large, direct substituent spin−orbit contributions. In view of an unexpectedly large gauge dependence of the **g**-tensor orientation in several cases, a recently developed implementation of gauge-including atomic orbitals (GIAO) has been applied.

1. Introduction

Galactose oxidase (GO) is an extracellular mononuclear copper enzyme isolated from culture media of a number of fungal species. It catalyzes the two-electron oxidation of primary alcohols to the corresponding aldehydes,[1,2] thereby reducing dioxygen to hydrogen peroxide. The fact that a single copper center is able to catalyze a two-electron reaction has been traced back to the presence of a protein radical. The latter is coordinated to the copper center and couples antiferromagnetically with Cu^{II} to a singlet state.[3] Although this active state is EPR-silent, the oxidized apo-enzyme could be studied by EPR spectroscopy (both at the X-band and at 139.5 GHz).[4−6] With the help of X-ray structural data,[7] the protein radical has been identified as being derived from a modified tyrosine that is covalently cross linked in the ortho position to the protein via a thioether function to a cystein residue (cf. Figure 1).[3,5,6] The EPR parameters of this tyrosyl radical differ from those of other tyrosyl radicals (e.g., those in ribonucleotide reductase). In particular, the largest component of the **g** tensor, g_x, is reduced, but g_y is increased. This results in an almost axially symmetric tensor.[5,6] A similar tensor was found for the model system 3-methylthiocresyl (MTC) in aqueous solution.[5,6] Nature may have designed the covalent cross link to modify the redox potential and thus the electron-transfer characteristics of the tyrosyl radical. In this context, it is necessary to know whether the ortho cysteine substituent has a significant influence on the spin density and **g** tensor of the radical.

In view of the relatively complicated nature of the electronic **g** tensor, its analysis by quantum chemical calculations is desirable to be able to relate spectroscopic information to the spin-density distribution. Until recently, theoretical studies were restricted to rather approximate, semiempirical models that have mainly supplied qualitative information. The development of more accurate ab initio and density functional theory (DFT) methods during the past 5−7 years has changed the situation significantly, and quantitative analyses and predictions have become possible.[8] Engström et al. have recently applied their ab initio multiconfiguration self-consistent-field (MCSCF) linear response formalism[9] not only to the study of hydrogen-bonding effects on the **g** tensor of the phenoxyl radical[10] but also to describe the **g** tensor of the substituted tyrosyl radical in GO (by studying an *o*-SH-substituted phenoxyl model).[11] An earlier DFT-based comparison between *o*-methylthio-cresyl and cresyl models by Gerfen et al.[6] had suggested very large changes in the spin-density distribution and **g** tensors due to the thioether substituent. In contrast, Engström et al. concluded that the influence of the sulfur substituent is small.[11]

The calculations of Gerfen et al. used Kohn−Sham orbitals obtained in local spin-density calculations.[6] Their reported spin-density distributions differ significantly from those obtained in other DFT studies[12−14] (see also ref 15). In particular, a very high spin density on sulfur was predicted. Moreover, Gerfen et al. applied a number of severe approximations in the perturbation procedure (one-center approximation to both spin−orbit and orbital-Zeeman matrix elements[16]) that render the **g**-tensor calculations at most semiquantitative (the results for cresyl differ significantly from experiment[6]). However, the agreement of the MCSCF **g**-tensor results[11] with experiment also is modest. The calculations reproduce well neither the experimentally observed[4,6] reduction of the g_x component nor the appreciable increase of the g_y component compared to unsubstituted tyrosyl. We suspect that, in view of the large computational effort

* Corresponding author. E-mail: kaupp@mail.uni-wuerzburg.de.
† Universität Würzburg.
‡ Slovak Academy of Sciences.

10.1021/jp026596p CCC: $25.00
Published on Web 12/10/2002

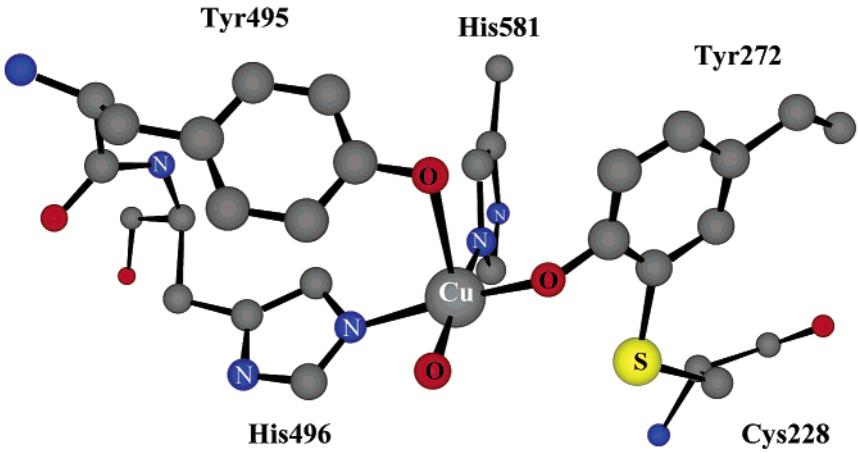

Figure 1. Modified tyrosine Tyr272 in galactose oxidase (cf. ref 7).

involved in the MCSCF procedure, the active orbital space was too restricted, and possibly the one-particle basis set was also too small.

In view of the contradictory results of the previous theoretical studies, we have decided to revisit the problem of the **g** tensor of the tyrosyl radical in GO using our own recent DFT approach[17] for the calculation of **g** tensors. Our DFT method does not suffer from the approximations used in ref 6. It has been shown to provide accurate **g** tensors for a large variety of radicals including semiquinone radical anions,[18,19] nitroxide spin labels,[20] and a number of phenoxyl radicals.[17] In particular, substituent effects and the influence of H bonding on the **g** tensors of semiquinone radical anions have been reproduced quantitatively.[18,19] Similarly, the comparison of unsubstituted phenoxyl, tyrosyl, and 2,4,6-tris-*tert*-butyl-phenoxyl radicals has provided good agreement with experiment for the substituted systems and has indicated significant substituent effects of the *tert*-butyl substituents in the latter species (due to hyperconjugation).[17] Because of its much lower computational cost compared to that of post-Hartree−Fock ab initio methods, the DFT approach may be easily applied to more realistic model systems, and it is applicable to a more general survey of different radicals. Here we compare phenoxyl and cresyl radicals with 3-methylthio-phenoxyl (MTP) and 3-methylthio-cresyl (MTC) as well as with the series of 2-XH-substituted phenoxyls (X = O, S, Se, Te). A detailed breakdown of **g**-shift components into atomic contributions is provided, and the relation of the **g** tensors to spin-density distributions is discussed. We also include hydrogen-bonded model systems.

2. Computational Details

Structure Optimizations. All structures have been optimized at the gradient-corrected DFT level (BP86 functional[21]) using the Gaussian 98 program.[22] The optimizations employed effective core potentials (ECPs) and DZP valence basis sets for the non-hydrogen atoms[23] and a DZV hydrogen basis.[24] The optimized dimensions are similar to those obtained in other studies of phenoxyl radicals.[12−14] On the basis of previous experience,[25] we expect that DFT optimizations will overestimate the bond lengths to the heavier chalcogen atoms S, Se, and Te by ca. 0.05 Å. Test calculations with artificially reduced bond lengths (data not shown) indicate that this will not affect any of the conclusions of the study. The chalcogen substituents are generally found to be coplanar with the phenoxyl ring. For models with XH substituents, we have optimized those conformers in which the hydrogen substituent points away from the phenoxyl oxygen atom to avoid intramolecular hydrogen bonding. In the hydrogen-bonded model complex MTC(H_2O), the more stable structure with the intermolecular hydrogen bond pointing away from the methylthio substituent has been considered in the **g**-tensor calculations. The reported Mulliken spin densities are based on the Gaussian 98 results.

g-Tensor Calculations. For an easier discussion of substituent effects, we report **g**-shift tensors $\Delta\mathbf{g}$, defined as $\Delta\mathbf{g} = \mathbf{g} - g_e\mathbf{1}$ ($g_e = 2.0023219$), in ppm (i.e., in units of 10^{-6}). Up to the level of second-order perturbation theory, the **g** shift $\Delta\mathbf{g}$ consists of the relevant Breit−Pauli terms[26]

$$\Delta\mathbf{g} = \Delta\mathbf{g}_{SO/OZ} + \Delta\mathbf{g}_{RMC} + \Delta\mathbf{g}_{GC}$$

of which the "paramagnetic" second-order spin−orbit/orbital-Zeeman cross term $\Delta\mathbf{g}_{SO/OZ}$ dominates (except for the smallest $\Delta\mathbf{g}$ values). Our method employs second-order perturbation theory based on Kohn−Sham calculations. Details of the method have already been discussed elsewhere.[17] The main advantage of our approach is the use of accurate and efficient approximations to the one- and two-electron spin−orbit matrix elements occurring in the $\Delta\mathbf{g}_{SO/OZ}$ term. In this work, we employed the all-electron atomic mean-field approximation (AMFI)[27,28] (cf. ref 17). The effectively atomic nature of the AMFI SO operators allows for the convenient breakdown of the computed $\Delta\mathbf{g}_{SO/OZ}$ components into atomic or fragment contributions by setting the SO operators for specific atoms or groups equal to zero.

The unrestricted Kohn−Sham calculations employed the deMon program,[29] and the perturbation calculations used the associated **g**-tensor module.[17] Most of the details of the calculations are the same as in our previous studies of semiquinone and phenoxyl radicals.[17−19] We used the uncoupled DFT level with the gradient-corrected BP86 functional[21] and DZVP basis sets.[24] Auxiliary basis sets for the fits of the exchange-correlation potential and the charge density were of sizes 5, 4 for S, 5, 5 for Se and Te, 5, 2 for C, N, and O, and 5, 1 for H (*n*, *m* denotes *n* s functions and *m* spd shells with shared exponents).[29] A compromise strategy discussed earlier[30] was applied to obtain accurate Kohn−Sham MOs with moderate effort by adding an extra iteration with a larger integration grid and without the fit of the exchange-correlation potential after initial SCF convergence has been reached. FINE angular grids with 64 points of radial quadrature were used. Unless stated otherwise, a common gauge at the center of nuclear charges was employed. Test calculations with other choices of gauge indicated little gauge dependence of the magnitude of the **g**-tensor components. However, surprisingly, in a number of

TABLE 1: Calculated *g*-Shift Components (in ppm) for Selected Phenoxyl Radicals Compared to Experiment

	Δg_{iso}	Δg_x	Δg_y	Δg_z
phenoxyl[a]	3680	8773	2286	21
tyrosyl	3493	7831	2183	55
cresyl[b]	3303	7861	2098	−51
cresyl (H_2O)	2865	6474	2148	−28
cresyl ($H_2O)_2$	2501	5469	2072	−37
exp, *N*-acetyl-Tyr (crystal)[c]	3300	7100		
exp, Tyr in *E. coli* RNR[d]	2990	6800	2250	−70
exp, Tyr_D in spinach PS-II[e]	2250	5240	2000	−170
exp, Tyr(HCl)[f]	1910	4260	1720	−240
o-SH−PhO[g]	3466	6203	4227	−33
o-SCH_3−PhO	3642	6142	4845	−61
MTC[h]	3506	5723	4820	−24
MTC (H_2O)	3329	5436	4590	−37
MTC ($H_2O)_2$	3220	5181	4527	−47
exp, apo-GO[i]	2990	5090	4090	−210
exp, MTC (in H_2O)[i]	2780	4880	3880	−420

[a] Previous MCSCF results (in ppm) for phenoxyl:[11] $\Delta g_x = 6400$, $\Delta g_y = 2700$, $\Delta g_z = 200$. [b] Previous DFT results for cresyl (in ppm):[6] $\Delta g_x = 14\,720$, $\Delta g_y = 1030$, $\Delta g_z = 0$. [c] Reference 37; no hydrogen bonding. [d] Reference 6; presumably no hydrogen bonding. [e] Reference 32; presumably hydrogen bonding. [f] Reference 36; hydrogen bonding. [g] Previous MCSCF results (in ppm) for *o*-SH−PhO:[11] $\Delta g_x = 5600$, $\Delta g_y = 2900$, $\Delta g_z = 200$. [h] Previous DFT results for MTC (in ppm):[6] $\Delta g_x = 3730$, $\Delta g_y = 2040$, $\Delta g_z = 0$. [i] Reference 6.

cases, a significant gauge dependence of the **g**-tensor orientation was observed. This point will be addressed further below.

3. Results and Discussion

Table 1 compares calculated **g**-shift tensors for various phenoxyl models with experimental data for (a) unsubstituted tyrosyl radicals in various environments[31−38] and (b) systems with thio substitution at the 3 position, such as the apo-GO tyrosyl radical[6] and the MTC radical in aqueous solution.[4,6] It is well known[39] that hydrogen bonding reduces in particular g_x (to some extent, also g_y) in π radicals such as phenoxyls,[10,31−38] semiquinones,[18,39,40] or nitroxides.[20] As models for tyrosyl in a protic environment, we have included complexes of cresyl with one or two water molecules hydrogen bonded to the phenoxyl oxygen. The calculated decrease in Δg_x by ca. 17 and 30% due to one and two hydrogen bonds, respectively, may be compared to tyrosyl radicals in biological or in vitro surroundings, which are presumably without or with hydrogen-bonding interactions. For example, the decrease from Tyr in *E. coli* RNR (where hydrogen bonding is thought to be absent[6,38]) or *N*-acetyl-tyrosyl crystal[37] to Tyr_D in PS-II (where at least one hydrogen bond is thought to be present[32,38]) is ca. 25%.

Allowing for an expected systematic overestimate of Δg_x by ca. 10% with the present gradient-corrected DFT method (as found for various semiquinones[18,19] and other phenoxyls[17]), we find the cresyl models to reproduce the **g** tensors of tyrosyl radicals well, as also seen from the direct computational comparison between cresyl and tyrosyl (Table 1). The smaller Δg_y components also agree well (experimental uncertainties of ca. ±100 ppm have to be taken into account). The much lower g_x and g_y in tyrosyl hydrochloride crystals[36] may reflect the additional electrostatic interactions present.

Turning to the sulfur-substituted systems (Table 1), we note that any of the models reproduces the experimentally observed lower Δg_x and larger Δg_y and thus the less pronounced rhombicity of the **g** tensor compared to that of the systems without sulfur. The SH substituent gives a somewhat lower Δg_y than the methylthio group. The para-methyl group in MTC reduces Δg_x compared to that in MTP, as seen also for cresyl or tyrosyl versus phenoxyl. ENDOR data for the modified tyrosyl radical in apo-GO suggest one hydrogen bond to be present (whereas in the active form of the enzyme the phenoxyl oxygen atom coordinates to the copper center).[5] We may expect up to two hydrogen bonds for MTC in aqueous solution. Given the fact that our calculations do not include possible π stacking to a Trp residue in apo-GO,[7] dielectric effects, or T-stacked[19] hydrogen bonding for MTC in solution, the agreement of the MTC(H_2O) and MTC($H_2O)_2$ model results with available experimental data may also be considered reasonable. Overall, the present calculations reproduce the experimentally observed[5,6] influence of the thio substituents remarkably well, much better than previous DFT or MCSCF calculations (cf. footnotes to Table 1). We may thus proceed to analyze the electronic origin of the substituent effects in more detail.

TABLE 2: Atomic Breakdown of *g*-Shift Components for Cresyl (in ppm)[a]

	Δg_{xx}	Δg_{xy}	Δg_{xz}	Δg_{yx}	Δg_{yy}	Δg_{yz}	Δg_{zx}	Δg_{zy}	Δg_{zz}
O	8232	−2	1	16	1805	1	0	1	−10
C1	86	−15	0	2	128	0	0	0	0
C2,6	−121	0	0	−5	−5	0	0	0	−3
C3,5	−308	10	0	6	230	0	0	0	2
C4	−9	1	0	3	30	0	0	0	2
C(CH3)	−2	−11	0	1	21	0	0	0	−3
total	7878	−20	1	25	2057	1	0	1	−11

[a] In general axes, cf. Figure 2.

TABLE 3: Atomic Breakdown of *g*-Shift Components for MTC (in ppm)[a]

	Δg_{xx}	Δg_{xy}	Δg_{xz}	Δg_{yx}	Δg_{yy}	Δg_{yz}	Δg_{zx}	Δg_{zy}	Δg_{zz}
O	4574	271	0	62	1426	0	0	0	−7
C1	56	−6	0	16	82	0	0	0	−0
C2	−24	−14	0	−3	−29	0	0	0	−1
C3	−13	−189	0	−167	102	0	0	0	0
C4	−41	63	0	142	97	0	0	0	1
C5	−50	10	0	−31	40	0	0	0	0
C6	−52	−19	0	14	22	0	0	0	−2
PhO	4451	115	0	34	1741	0	0	0	−10
C(CH3)	2	10	0	2	12	0	0	0	−2
S	1188	−402	−1	−176	3026	0	0	0	−33
C(SCH3)	6	7	0	6	4	0	0	0	−2
total	5646	−271	−1	−135	4782	0	0	0	−47

[a] $\Delta g_{SO/OZ}$ in general axes, cf. Figure 2.

The one-center nature of the AMFI SO operators employed allows a breakdown of the $\Delta g_{SO/OZ}$ term into atomic or fragment contributions[17] (as attempted in ref 6 for cresyl and MTC on a much less quantitative basis). Because of the fact that the sulfur SO contributions change the orientation of the principal axes of the tensor (see below), we discuss the results (Tables 2 and 3) in the general axis system shown in Figure 2. In this framework, the sulfur SO coupling leads to nonnegligible off-diagonal contributions Δg_{xy} and Δg_{yx}, which are partially lost when transforming to the principal axis system of the full tensor (note also the inherently unsymmetrical nature of the **g** matrix).

For cresyl (Table 2), the analysis shows the usual dominance of the oxygen contribution but with nonnegligible contributions from the carbon atoms, as discussed previously for phenoxyl.[17] Sulfur substitution in MTC (Table 3) reduces the oxygen contributions, in particular to Δg_{xx} but also to Δg_{yy}. The reduced oxygen contributions to Δg_{xx} are partially compensated by significant direct sulfur SO contributions. For Δg_{yy}, the sulfur contributions overcompensate for the loss of oxygen SO coupling, and thus Δg_{yy} is increased compared to the value for cresyl. Together with the further reduction of Δg_x by hydrogen bonding (cf. MTC(H_2O)), this explains the almost axially

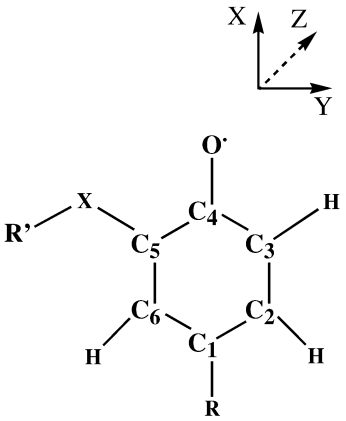

Figure 2. Axis system and atom labeling employed for substituted phenoxyl radicals.

TABLE 4: Mulliken Spin Densities (in au)[a]

atom	cresyl[b]	MTC[c]
O	0.39 (0.39)	0.31 (0.31)
C1	0.38 (0.35)	0.32 (0.28)
C2	−0.13 (−0.10)	−0.12 (−0.10)
C3	0.27 (0.26)	0.24 (0.23)
C4	−0.07 (−0.05)	−0.02 (0.00)
C5	0.30 (0.26)	0.20 (0.18)
C6	−0.13 (−0.10)	−0.07 (−0.05)
S		0.14 (0.14)
$C(SCH_3)$		0.00
$C(CH_3)$	−0.03	−0.02

[a] Taken from the output of the ECP structure optimizations using the BP86 functional. Compare to Figure 2 for atom numbering. [b] BLYP results for tyrosyl from ref 13 given in parentheses. [c] BLYP results for *o*-EtS-tyrosyl from ref 13 given in parentheses.

symmetric tensor. Substitution also modifies the carbon contributions. For example, the C4 contributions are enhanced, and off-diagonal contributions from C3 or C4 appear in the general axis system. The change in the overall tensor orientation will be discussed further below.

The changes in the oxygen and carbon contributions as well as the magnitude of the direct sulfur contributions may be traced back to a modified spin-density distribution. Table 4 compares Mulliken atomic spin densities in cresyl and MTC. Obviously, sulfur substitution damps the spin-density alternation in the odd−even π radical. This partially explains, for example, the reduced oxygen and C4 contributions to the **g** tensor. The computed spin-density distribution is very similar to those obtained in previous DFT studies with gradient-corrected functionals (cf. BLYP results from ref 13 in Table 4). Hybrid functionals give an even slightly lower spin density on sulfur and a slightly larger spin density on oxygen.[13] The present calculations thus allow us to relate realistic spin-density distributions in detail to accurate estimates of contributions to $\Delta g_{SO/OZ}$.

As our method does not rely on semiempirical SO operators, we may also straightforwardly extend our study to substituents from lower rows in the periodic table. Table 5 compares computed **g**-shift tensors for a series of *o*-XH-substituted phenoxyl radicals. The Δg_x and Δg_y components along this series are shown graphically in Figure 3. Δg_x remains almost constant and below the value for unsubstituted phenoxyl for X = O, S before increasing sharply with X = Se, Te. In contrast, Δg_y is below the value for the unsubstituted system (dotted horizontal line) for X = O but already significantly above it for X = S. The approximate breakdown into fragment contributions (an exact breakdown may be made in the general axes; cf. Supporting Information) reveals the origin of the different trend for the two components: The phenoxyl oxygen contribution to Δg_x is reduced significantly by substitution and increasingly so with heavier X substituents (Figure 3a). The direct SO contribution from X = S is too small to compensate for this decrease, and only with X = Se does the large selenium SO contribution start to dominate Δg_x. In contrast, the reduction of the phenoxyl (mainly oxygen) contribution to Δg_y is less pronounced, and it is already easily overcompensated by the substituent SO contribution starting with X = S (Figure 3b). It is notable that our calculations predict very large positive Δg_x and Δg_y values for selenium and tellurium substituents. There appear to be no experimental data for phenoxyl radicals substituted with these heavy chalcogens. However, it is known, for example, for tetrahalogen-substituted semiquinone radical anions[41] (see also ref 40), that heavy halogen substituents may lead to large positive Δg values. In addition to the larger SO coupling constants for the heavier chalcogen substituents, the very large increase in both g_x and g_y is also partially due to an increase in spin density on the substituent atoms (Mulliken spin densities of 0.086, 0.130, 0.145, and 0.165 are computed for X = O, S, Se, and Te, respectively). The monotonic decrease of the phenoxyl fragment contribution to Δg_x (Figure 3a) may in turn be traced back to decreasing spin density on the phenoxyl oxygen atom.

TABLE 5: Calculated *g*-Shift Components (in ppm) of ortho-Chalcogen-Substituted Phenoxyl Radicals[a]

XR	Δg_{iso}	Δg_x	Δg_y	Δg_z
H[b]	3680	8773	2286	21
OH	2920	6425	2391	−56
SH	3466	6204	4227	−32
SeH	8631	17 553	8423	−84
TeH	16 743	40 187	10 076	−34

[a] All-electron AMFI results. [b] Unsubstituted phenoxyl.

Table 6 summarizes the angles that the g_x principal axes form with the C−O bond vector (i.e., with the *x* axis in Figure 2). Although the magnitude of Δg_x or Δg_y tends to vary only up to ca. 5% upon moving the gauge origin of the magnetic vector potential (however, a common gauge on the phenoxyl oxygen atom may lead to as much as a 10% lower Δg_y), we found, surprisingly, that the sulfur-substituted systems exhibit a significant gauge dependence of the orientation of the two components within the *xy* plane. Thus, whereas calculations with the gauge origin at the center of nuclear charges (typically located within the phenoxyl ring, slightly shifted toward the substituent) or at the phenoxyl oxygen atom gave a very large reorientation of Δg_x away from the phenoxyl C−O bond vector, a gauge origin at the sulfur atom provided significantly smaller angles. Notably, this extreme gauge dependence is found for the sulfur-substituted systems (and to some extent for the small reorientation angles of the OH-substituted system) but not for the Se- or Te-substituted phenoxyls. Previous work by several groups had suggested that the **g** tensor is only very moderately gauge-dependent.[8] The present study suggests that this does not hold for the orientation of the tensor if spin−orbit contributions from different parts of the molecule compete for control of the preferred orientation. In the sulfur-substituted phenoxyls, it is the sulfur atom and the phenoxyl oxygen atom that make substantial contributions to $\Delta g_{SO/OZ}$, with noticeably different orientational preferences.

In this situation, distributed-gauge methods are preferable over a common gauge origin. We have previously employed individual gauges for localized orbitals (IGLO[42]). However, because of artifacts arising during the separate localization of alpha and

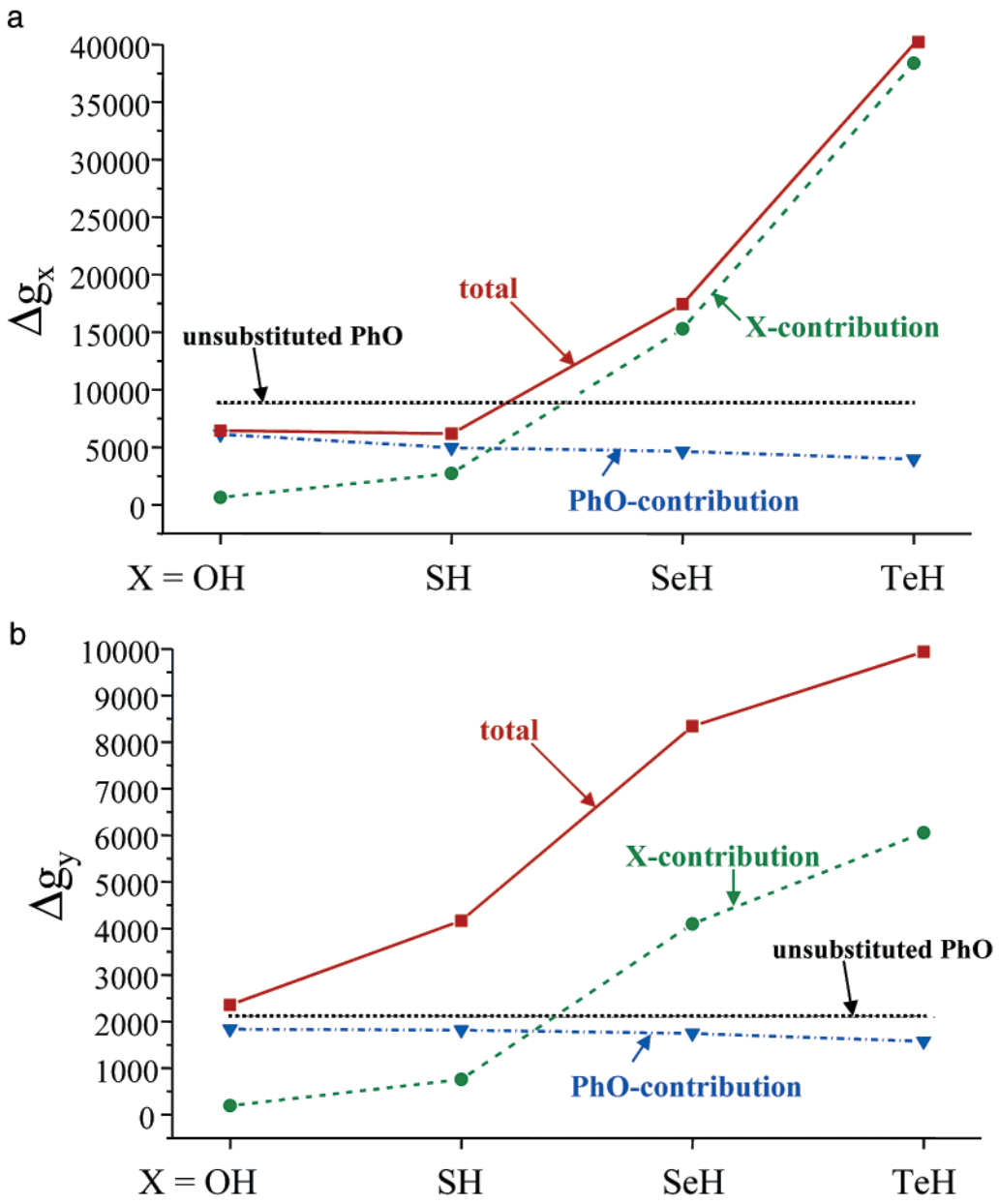

Figure 3. Fragment contributions to Δg in ortho-chalcogen-substituted phenoxyl radicals: (a) Δg_x, (b) Δg_y. Because of the occurrence of nondiagonal elements, the XH and PhO contributions do not add up completely to the full tensor components in the principal axis system (see text).

TABLE 6: Angles (in degrees) of g_x Principal Tensor Axes with the Phenoxyl C−O Bond Vector[a]

phenoxyl	0.0, 0.0, −	cresyl(H_2O)	3.6, 2.5, −	*o*-OH−PhO	5.1, 5.3, 2.4
cresyl	0.1, 0.0, −	cresyl(H_2O)$_2$	0.2, 0.2, −	*o*-SH−PhO	19.0, 17.7, 12.2
MTP	14.3, 16.4, 1.4	MTC(H_2O)	36.8, 28.2, 12.5	*o*-SeH−PhO	27.9, 31.1, 27.7
MTC	13.5, 17.6, 1.8	MTC(H_2O)$_2$	38.1, 30.8, 10.6	*o*-TeH−PhO	72.5, 71.2, 73.0

[a] Compare with Figure 2 for general axis system. Results are provided for three different choices of gauge origin: (a) center of nuclear charges, (b) phenoxyl oxygen atom, and (c) heavy-substituent atom.

beta spin orbitals, this approach turned out[18] to be only partially suitable in such cases as the delocalized phenoxyl radicals studied here. Gauge-including atomic orbitals (GIAOs[43]) are the preferred method in this case.[44] We have recently implemented GIAOs into our new property code MAG-ReSpect.[45] As the combination of GIAOs with the AMFI approximation for the SO operators has not yet been completed, we have carried out calculations with a computationally more demanding explicit evaluation of the one- and two-electron SO integrals. The calculated angles between the Δg_x principal axis and the *x*-direction are 2.9, 4.8, 15.1, 14.1, and 15.0° for MTP, MTC, MTC(H_2O), MTC(H_2O)$_2$, and *o*-SH−PhO, respectively. These results are intermediate between the larger angles obtained with the gauge origin on the phenoxyl oxygen atom (Table 6) and the smaller angles with the gauge origin on the sulfur atom, but they tend to be closer to the latter. Consequently, our GIAO results are intermediate between the MCSCF data of 8°, which Engström et al. obtained for *o*-SH−PhO,[11] and the larger 23° angle that Gerfen et al. obtained in DFT calculations for MTC.[6] Notably, both previous works were carried out with a common gauge origin (not specified in ref 6, probably at the center of charge in ref 11). In view of the present results, this is not

sufficient to allow for a meaningful discussion of the tensor orientation. We regard the current DFT-GIAO results as the most accurate estimate for the angles. However, the angles for the various sulfur-substituted systems are notably different. It appears that the actual angle in these particular systems is influenced significantly by the precise nature of the substituents as well as by hydrogen bonding.

For the hypothetical *o*-SeH−PhO and *o*-TeH−PhO, both g_x and g_y are dominated by direct SO contributions from the heavy chalcogen atoms (Table 5, Figure 3). Therefore, the gauge dependence of the tensor orientation is much less pronounced than for the sulfur-substituted phenoxyls (Table 6; GIAO calculations provide similar results). The results show clearly that the large, positive $\Delta g_{SO/OZ}$ contributions to both g_x and g_y are accompanied by a substantial reorientation of the two components compared to that of unsubstituted phenoxyl. In the tellurium-substituted system, the larger g_x component is oriented parallel to the C3−Te bond vector.

4. Conclusions

Although the modified radical in GO is still characterizable as a typical tyrosyl species with an even−odd alternating spin-density distribution, the influence of sulfur substitution on the spin density and **g** tensor is far from negligible. The present calculations reproduce the experimentally observed substituent effects on the magnitude of the **g**-tensor components quantitatively and could thus be used to analyze the relation between the **g** tensor and the electronic structure in more detail than possible previously. The overall relatively small substituent effect on the g_x component is due to a partial cancellation between the reduced oxygen and direct sulfur spin−orbit contributions. The enhanced g_y is due to direct sulfur contributions. Hydrogen bonding reduces g_x further and thus renders g_x and g_y even more similar to each other, leading to an almost axially symmetric tensor. Large spin−orbit contributions from heavier chalcogen substituents such as selenium and tellurium are predicted to enhance g_x and g_y components dramatically and to change the tensor orientation fundamentally. An unexpectedly large gauge dependence of the tensor orientation (not of the magnitude of the tensor components) was found for the sulfur-substituted phenoxyl radicals and could be attributed to a competition between sulfur and oxygen $\Delta g_{SO/OZ}$ contributions. The present results should aid in the interpretation of future EPR studies of substituted tyrosyl radicals by providing a direct link between observed **g** tensors and the spin-density distribution.

Despite the significant influence of the heavier chalcogen substituents on the **g** tensors, evidence has increasingly accumulated that a thioether cross link to tyrosine does not alter its O−H bond strength or the ionization potential of the tyrosinate substantially.[12−14,46] Similarly, DFT model calculations on individual steps in the catalytic mechanism of GO did not suggest any noticeable influence of sulfur substitution on the barriers or relative energies of intermediates.[47] The intramolecular electronic effect of the substituent thus is probably of minor importance to the function of the enzyme. Himo et al. suggested that the role of the cross link is a structural one.[47] Of course the cross link might also indirectly alter the electronic characteristics and thus the redox potential of the tyrosyl radical. Mutants lacking the cross link appear to bind copper less strongly to the active site.[48] In addition, the cross link could also serve to anchor Tyr272 in the crystallographically observed π-stacked arrangement with a nearby tryptophan residue[7] (Trp290, not shown in Figure 1). Further computational and experimental work will be needed to establish the actual role of the cross link in the function of galactose oxidase.

Acknowledgment. This study has been supported by the Deutsche Forschungsgemeinschaft (Priority Program SP1051, "High-Field EPR") and by Fonds der Chemischen Industrie. Part of this work benefitted also from the graduate college "Moderne Methoden der magnetischen Resonanz in der Materialforschung" at Universität Stuttgart. Financial support from the Slovak Grant Agency VEGA (grant no. 2/7203/20) and the COST Chemistry Program (D9/0002/97) is gratefully acknowledged by V.G.M., O.L.M., and R.R.

Supporting Information Available: A fragment breakdown of **g**-shift components for ortho-chalcogen-substituted phenoxyl radicals in a general axes system. This material is available free of charge via the Internet at http://pubs.acs.org.

References and Notes

(1) See, for example, Stubbe, J.; van der Donk, W. A. *Chem. Rev.* **1998**, *98*, 705. Klinman, J. P. *Chem. Rev.* **1996**, *96*, 2541.

(2) Whittaker, J. W. In *Metal Ions in Biological Systems;* Sigel, H., Sigel, A., Eds.; Marcel Dekker: New York, 1994; Vol. 30, pp 315−359.

(3) Whittaker, M. M.; Whittaker, J. W. *J. Biol. Chem.* **1988**, *263*, 6074.

(4) Whittaker, M. M.; Whittaker, J. W. *J. Biol. Chem.* **1990**, *265*, 9610.

(5) Babcock, G. T.; El-Deeb, M. K.; Sandusky, P. O.; Whittaker, M. M.; Whittaker, J. W. *J. Am. Chem. Soc.* **1992**, *114*, 3727.

(6) Gerfen, G. J.; Bellew, B. F.; Griffin, R. G.; Singel, D. J.; Ekberg, Ch. A.; Whittaker, J. W. *J. Phys. Chem.* **1996**, *100*, 16739.

(7) Ito, N.; Phillips, S. E. V.; Stevens, C.; Ogel, Z. B.; McPherson, M. J.; Keen, J. N.; Yadaf, K. D. S.; Knowles, P. F. *Nature (London)* **1991**, *350*, 87.

(8) For a recent review, see Kaupp, M. Ab Initio and Density Functional Calculations of Electronic g-Tensors for Organic Radicals. In *EPR Spectroscopy of Free Radicals in Solids: Trends in Methods and Applications;* Lund, A., Shiotani, M., Eds.; Kluwer: Dordrecht, The Netherlands, 2003.

(9) Vahtras, O.; Minaev, B.; Ågren, H. *Chem. Phys. Lett.* **1997**, *281*, 186.

(10) Engström, M.; Vahtras, O.; Ågren, H. *Chem. Phys.* **1999**, *243*, 263.

(11) Engström, M.; Himo, F.; Ågren, H. *Chem. Phys.* **2000**, *319*, 191.

(12) Wise, K. E.; Pate, J. B.; Wheeler, R. A. *J. Phys. Chem. B* **1999**, *103*, 4764.

(13) Himo, F.; Babcock, G. T.; Eriksson, L. A. *Chem. Phys. Lett.* **1999**, *313*, 374.

(14) Himo, F.; Eriksson, L. A.; Blomberg, M. R. A.; Siegbahn, P. E. M. *Int. J. Quantum Chem.* **2000**, *76*, 714.

(15) A different view is provided by Boulet, A. M.; Walter, E. D.; Schwartz, D. A.; Gerfen, G. J.; Callis, P. R.; Singel, D. J. *Chem. Phys. Lett.* **2000**, *331*, 108.

(16) Stone, A. J. *Proc. R. Soc. London, Ser. A* **1963**, *271*, 424.

(17) Malkina, O. L.; Vaara, J.; Schimmelpfennig, B.; Munzarová, M.; Malkin, V. G.; Kaupp, M. *J. Am. Chem. Soc.* **2000**, *122*, 9206.

(18) Kaupp, M.; Remenyi, C.; Vaara, J.; Malkina, O. L.; Malkin, V. G. *J. Am. Chem. Soc.* **2002**, *124*, 2709.

(19) Kaupp, M. *Biochemistry* **2002**, *41*, 2895.

(20) Owenius, R.; Engström, M.; Lindgren, M.; Huber, M. *J. Phys. Chem. A* **2001**, *105*, 10967. Engström, M.; Vaara, J.; Schimmelpfennig, B.; Ågren, H. *J. Phys. Chem. B* **2002**, *106*, 12354. Engström, M. Ph.D. Thesis, Linköpings Universitet, Sweden, 2001.

(21) Becke, A. D. *Phys. Rev. A* **1988**, *38*, 3098. Perdew, J. P.; Wang, Y. *Phys. Rev. B* **1986**, *33*, 8822.

(22) Frisch, M. J.; Trucks, G. W.; Schlegel, H. B.; Scuseria, G. E.; Robb, M. A.; Cheeseman, J. R.; Zakrzewski, V. G.; Montgomery, J. A., Jr.; Stratmann, R. E.; Burant, J. C.; Dapprich, S.; Millam, J. M.; Daniels, A. D.; Kudin, K. N.; Strain, M. C.; Farkas, O.; Tomasi, J.; Barone, V.; Cossi, M.; Cammi, R.; Mennucci, B.; Pomelli, C.; Adamo, C.; Clifford, S.; Ochterski, J.; Petersson, G. A.; Ayala, P. Y.; Cui, Q.; Morokuma, K.; Malick, D. K.; Rabuck, A. D.; Raghavachari, K.; Foresman, J. B.; Cioslowski, J.; Ortiz, J. V.; Stefanov, B. B.; Liu, G.; Liashenko, A.; Piskorz, P.; Komaromi, I.; Gomperts, R.; Martin, R. L.; Fox, D. J.; Keith, T.; Al-Laham, M. A.; Peng, C. Y.; Nanayakkara, A.; Gonzalez, C.; Challacombe, M.; Gill, P. M. W.; Johnson, B. G.; Chen, W.; Wong, M. W.; Andres, J. L.; Head-Gordon, M.; Replogle, E. S.; Pople, J. A. *Gaussian 98*, revisions A.7 and A.9; Gaussian, Inc.: Pittsburgh, PA, 1998.

(23) (a) Bergner, A.; Dolg, M.; Küchle, W.; Stoll, H.; Preuss, H. *Mol. Phys.* **1993**, *80*, 1431. (b) d-Type polarization functions have been taken

from *Gaussian Basis Sets for Molecular Calculations;* Huzinaga, S., Ed.; Elsevier: New York, 1984.

(24) Godbout, N.; Salahub, D. R.; Andzelm, J.; Wimmer, E. *Can. J. Chem.* **1992**, *70*, 560.

(25) See, for example, Kaupp, M. *Chem. Ber.* **1996**, *129*, 535. Altmann, J. A.; Handy, N. C.; Ingamells, V. E. *Mol. Phys.* **1997**, *92*, 339.

(26) Harriman, J. E. *Theoretical Foundations of Electron Spin Resonance*; Academic Press: New York, 1978.

(27) Hess, B. A.; Marian, C. M.; Wahlgren, U.; Gropen, O. *Chem. Phys. Lett.* **1996**, *251*, 365.

(28) The AMFI code used is due to Schimmelpfennig, B. *Atomic Spin−Orbit Mean-Field Integral Program*; Stockholms Universitet: Sweden, 1996.

(29) (a) Salahub, D. R.; Fournier, R.; Mlynarski, P.; Papai, I.; St-Amant, A.; Ushio, J. In *Density Functional Methods in Chemistry*; Labanowski, J., Andzelm, J., Eds.; Springer: New York, 1991. (b) St-Amant, A.; Salahub, D. R. *Chem. Phys. Lett.* **1990**, *169*, 387.

(30) Malkin, V. G.; Malkina, O. L.; Eriksson, L. A.; Salahub, D. R. In *Modern Density Functional Theory: A Tool for Chemistry;* Seminario, J. M., Politzer P., Eds.; Theoretical and Computational Chemistry Series; Elsevier: Amsterdam, 1995; Vol. 2.

(31) Un, S.; Atta, M.; Fontcave, M.; Rutherford, A. W. *J. Am. Chem. Soc.* **1995**, *117*, 10713. Un, S.; Tang, X.-S., Diner, B. A. *Biochemistry* **1996**, *35*, 679.

(32) Dorlet, P.; Rutherford, A. W.; Un, S. *Biochemistry* **2000**, *39*, 7826.

(33) van Dam, P. J.; Willems, J.-P.; Schmidt, P. P.; Pötsch, S.; Barra, A.-L.; Hagen, W. R.; Hoffman, B. M.; Andersson, K. K.; Gräslund, A. *J. Am. Chem. Soc.* **1998**, *120*, 5080. Schmidt, P. P.; Andersson, K. K.; Barra, A.-L.; Thelander, L.; Gräslund, A. *J. Biol. Chem.* **1996**, *271*, 23615.

(34) Gerfen, G. J.; Bellew, B. F.; Un, S.; Bollinger, J. M.; Stubbe, J., Griffin, R. G. *J. Am. Chem. Soc.* **1993**, *115*, 6420. Berthomieu, C.; Hienerwald, R.; Boussac, A.; Diner, B. A. *Biochemistry* **1998**, *37*, 10547.

(35) Ivancich, A.; Mattioli, T. A.; Un, S. *J. Am. Chem. Soc.* **1999**, *121*, 5743. Allard, P.; Barra, A. L.; Andersson, K. K.; Schmidt, P. P.; Atta, M.; Gräslund, A. *J. Am. Chem. Soc.* **1996**, *118*, 895. Un, S.; Gerez, C.; Elleingard, E.; Fontecave, M. *J. Am. Chem. Soc.* **2001**, *123*, 3048. Ivancich, A.; Dorlet, P.; Goodin, D. B.; Un, S. *J. Am. Chem. Soc.* **2001**, *123*, 5050, and references cited in these works.

(36) Fasanella, E. L.; Gordy, W. *Proc. Natl. Acad. Sci. U.S.A.* **1969**, *62*, 299.

(37) Mezzetti, A.; Maniero, A. L.; Brustolon, M.; Giacometti, G.; Brunel, L. C. *J. Phys. Chem. A* **1999**, *103*, 9636.

(38) See also Un, S.; Dorlet, P.; Rutherford, A. W. *Appl. Magn. Reson.* **2001**, *21*, 341.

(39) Stone, A. J. *Mol. Phys.* **1963**, *6*, 509. Stone, A. J. *Mol. Phys.* **1964**, *7*, 311.

(40) Knüpling, M.; Törring, J. T.; Un, S. *Chem. Phys.* **1996**, *219*, 291, and references therein.

(41) Brabhanda, B. S.; Felix, C. C.; Hyde, J. S. *J. Chem. Phys.* **1985**, *83*, 612.

(42) Kutzelnigg, W.; Fleischer, U.; Schindler, M. In *NMR*: *Basic Principles and Progress;* Diehl, P., Fluck, E., Günther, H., Kosfeld, R., Eds.; Springer-Verlag: Heidelberg, Germany, 1990; Vol. 23, pp.165ff.

(43) See, for example, Ditchfield, R. *Mol. Phys.* **1974**, *27*, 789. Wolinski, K.; Hinton, J. F.; Pulay, P. *J. Am. Chem. Soc.* **1990**, *112*, 8251.

(44) For alternative DFT-GIAO **g**-tensor approaches, see van Lenthe, E.; Wormer, P. E. S.; van der Avoird, A. *J. Chem. Phys.* **1997**, *107*, 2488. Schreckenbach, G.; Ziegler, T. *J. Phys. Chem. A* **1997**, *101*, 3388.

(45) Malkin, V. G.; Malkina, O. L.; Reviakine, R.; Schimmelpfennig, B.; Arbuznikov, A.; Kaupp, M. *MAG-ReSpect*, version 1.0, 2001.

(46) Whittaker, M. M.; Chuang, Y.-Y.; Whittaker, J. W. *J. Am. Chem. Soc.* **1993**, *115*, 10092.

(47) Himo, F.; Eriksson, L. A.; Maseras, F.; Siegbahn, P. E. M. *J. Am. Chem. Soc.* **2000**, *122*, 8031. See also Röthlisberger, U.; Carloni, P.; Doclo, K.; Parrinello, M. *J. Biol. Inorg. Chem.* **2000**, *5*, 236.

(48) Baron, A. J.; Stevens, C.; Wilmot, C.; Seneviratne, K. D.; Blakeley, V.; Dooley, D. M.; Phillips, S. E. V.; Knowles, P. F.; McPherson, M. J. *J. Biol. Chem.* **1994**, *269*, 25095.